

^{15}N photoneutron cross section

A. D. Bates, R. P. Rassool, E. A. Milne, and M. N. Thompson
School of Physics, University of Melbourne, Parkville 3052, Australia

K. G. McNeill

Physics Department, Toronto University, Toronto, Ontario, Canada M5S 1A7

(Received 15 September 1988)

Two independent measurements of the $^{15}\text{N}(\gamma, n)$ reaction cross section have been made using both an enriched-gas target, and one of $(^{15}\text{NH}_4)_2\text{SO}_4$. The results are self-consistent, but reveal discrepancies with an earlier measurement of this cross section, particularly in the giant dipole resonance region, and with a measurement of the $^{15}\text{N}(\gamma, n_0)$ cross section. These discrepancies are discussed and in general resolved. The results are used in conjunction with other isospin-selective reactions data on ^{15}N to elucidate the isospin distribution of $E1$ states in ^{15}N .

I. INTRODUCTION

As part of a series of measurements of the photoneutron cross sections of nuclei with one or two nucleons or holes outside a closed shell or subshell (see Ref. 1 and associated references), the total photoneutron cross section for ^{15}N was measured at Lawrence Livermore National Laboratory (LLNL).² For this nucleus, the $^{15}\text{N}(\gamma, n_0)$ (Ref. 3) and the inverse $^{14}\text{N}(n, \gamma_0)$ (Ref. 4) cross sections have also been measured.

Although these three cross sections for ^{15}N all agree in general, in detail there are some discrepancies. In particular, the $^{15}\text{N}(\gamma, n_0)$ cross section is significantly larger than the total photoneutron cross section in the excitation-energy region about 15 MeV. In order to resolve this discrepancy it was decided to remeasure the $^{15}\text{N}(\gamma, n)$ reaction cross section using the 35-MeV betatron in this laboratory. In so doing, a far more troubling disagreement with the LLNL data was revealed in the giant dipole resonance (GDR) region of the cross section. In fact, we have made two measurements of the cross section using different methods: one using a high-pressure ^{15}N -gas target, and the other using a sample of ^{15}N -enriched ammonium sulphate. Both measurements confirm that the GDR peaks at about 25 MeV rather than at 23 MeV as indicated by the LLNL measurement.²

Because the dominant decay channels for the photodisintegration of ^{15}N are now better known, it is possible to attempt a reconciliation between the structure seen in these various reaction channels with the known states in ^{15}N . This is done with particular emphasis on the isospin assignment of the states, using the cross section presented here together with other isospin-selective reactions. The subsequent resolving of the GDR of ^{15}N into its two isospin components allows comparison with theoretical predictions of their relative contributions to the absorption cross sections; the energy separation of these two components may also be compared with theoretical predictions.

II. EXPERIMENTAL DETAILS AND DATA ANALYSIS

Both measurements of the reaction cross section used the yield-curve method. Details of this technique and the neutron detector are given elsewhere,⁵ and only specific details will be given here. The Halpern-type 4π neutron detector consisted of two concentric rings, each containing eight ^{10}B -enriched BF_3 proportional counters embedded in a paraffin block. The dose was monitored using a thin-walled transmission chamber placed before the sample. This chamber was intercalibrated against a replica P2 ionization chamber.⁶ An energy calibration of the betatron was performed before each of the measurements. The uncertainty in the energy is estimated to be about 100 keV below 20 MeV increasing to about 150 keV at 28 MeV.

The fact that two measurements were made is a consequence of the chronology of the experiments. The first determination was using the ^{15}N -enriched ammonium sulphate sample, which was available and convenient. The use of a compound sample naturally resulted in a significant contribution to the neutron yield from sulphur and oxygen in addition to that from the ^{15}N . Although this background yield was carefully measured and allowed for, the significant disagreements with the earlier LLNL measurement, particularly in the GDR region, prompted us to remeasure the cross section with an elemental sample. The agreement between the two results tends to validate the experimental observations.

A. Measurement using a sample of ^{15}N -enriched ammonium sulphate

The sample was in the form of 108 g of $(\text{NH}_4)_2\text{SO}_4$ powder, enriched to 98% in ^{15}N , and contained in a lucite cylinder with an internal diameter of 37.9 mm and a length 101.6 mm. Because of the presence of nuclei other than ^{15}N , in order to deduce the yield curve of the desired reaction it was necessary to measure yield curves from both sulphur and oxygen samples in addition to that from

the compound sample. The sample used for this background measurement consisted of a suspension of 25.6 g of sulphur in 58.3 g of water contained in an identical lucite holder. These precise amounts were chosen to equal the amounts of these impurities in the foreground sample.

Both foreground and background yield curves were measured from 10.5 to 28.0 MeV in intervals of 100 keV [the $^{15}\text{N}(\gamma, n)$ threshold energy is 10.8 MeV]. A total of 26 independent foreground and 15 background curves was measured. After subtraction an average yield curve for the $^{15}\text{N}(\gamma, xn)$ reaction was deduced.

B. Measurement using a ^{15}N -gas target

In this determination of the $^{15}\text{N}(\gamma, n)$ reaction cross section, the same detector and dose measuring system was used as in the experiment described above. However, the 37-g sample was in the form of nitrogen gas, enriched to 98.9% in ^{15}N . It was contained in a steel cylinder 2170 mm long and 42.4 mm outer diameter with walls 2.77 mm thick. The beam was collimated so that it did not hit the walls of the container. The length of the container was such that the steel end pieces were outside the neutron detector, and thus made a negligible contribution to the detected neutron count rate. A simple calculation indicated that the contribution to the yield due to scattering by the sample of neutrons produced in the relatively thin end caps was less than 0.1% of the yield from the sample. The detection efficiency for the extended sample was measured to be 5.3%, and to be constant within 10% for neutrons with energies between 0.5 and 10 MeV. The neutron efficiency of the detector was determined both from measurements using calibrated neutron sources and from a measurement of the $D(\gamma, p)n$ reaction cross section.

The yield of photoneutrons from the sample was determined at bremsstrahlung energies ranging from 10 to 26.5 MeV. In the range from 10 to 19.5 MeV, yield points were taken at 100-keV intervals, and elsewhere at intervals of 200 keV. This gave a high resolution cross section in the energy region which prompted the measurement, while allowing a cross section to be determined in the region of, and above the GDR with reasonable resolution. A total of 37 independent yield curves was measured with the sample in, each taking 5 h. A total of 10 sample-out yield curves was measured. The yield from the evacuated container constituted about 15% of the sample-in yield over most of the energy range. From these two sets of data, average yield curves were obtained from the filled and empty container, which allowed the yield curve for the $^{15}\text{N}(\gamma, n)$ reaction to be determined by subtraction.

C. The resulting $^{15}\text{N}(\gamma, sn)$ reaction cross sections

For each experiment, the resulting net yield curve, corrected for photon-monitor response, dead-time effects, and including absolute scaling factors, was analyzed using the variable bin Penfold-Leiss (VBPL) method.⁷ The ability of the VBPL method in resolving structure below the GDR, and its reliability in reproducing correct cross section magnitudes above the GDR were established by

an experiment performed by Pywell *et al.*⁸ in this laboratory. The resulting $^{15}\text{N}(\gamma, xn)$ reaction cross section includes the $^{15}\text{N}(\gamma, n)$, $^{15}\text{N}(\gamma, pn)$, and twice the $^{15}\text{N}(\gamma, 2n)$ reaction cross sections. Allowance for the double counting of the $^{15}\text{N}(\gamma, 2n)$ reaction was made by subtracting the contribution of the $^{15}\text{N}(\gamma, 2n)$ reaction, which was recently measured at this laboratory.⁹ The resulting estimates of the $^{15}\text{N}(\gamma, sn)$ reaction cross section are shown in Fig. 1, Fig. 1(a) being that measured using the gas target. The cross section in the excitation region from threshold to 19.5 MeV was derived from the yield curve measured in 100-keV steps, and has better resolution than the remainder of the cross section up to 26.5 MeV, which was derived from the 200-keV yield curve. Figure 1(b) shows the $^{15}\text{N}(\gamma, sn)$ cross section measured using the $(\text{NH}_4)_2\text{SO}_4$ sample. The error bars in both cases indicate only the statistical uncertainty; there is an overall systematic uncertainty of about 8% in the case of Fig. 1(a). For the cross section shown in Fig. 1(b), the systematic uncertainty could be as large as 12%, mainly due to the effects associated with allowing for the contribution from background elements in the compound sample. The two estimates are similar in both magnitude and overall shape: detailed agreement is good, bearing in mind the uncertainties discussed above.

Of particular interest is the agreement as to the posi-

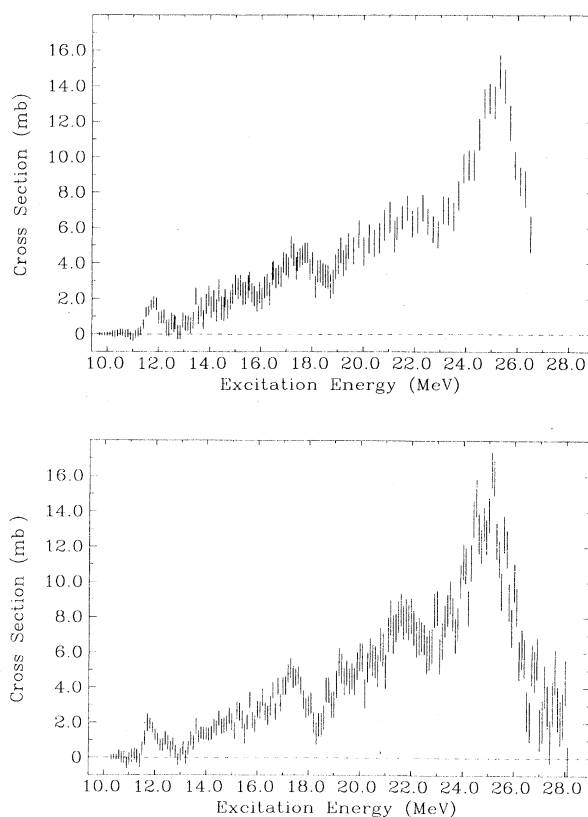


FIG. 1. The $^{15}\text{N}(\gamma, sn)$ reaction cross section: the upper figure shows the results obtained using a high-pressure ^{15}N -enriched gas sample, and the lower figure shows the results obtained using a solid $(\text{NH}_4)_2\text{SO}_4$ sample.

tion (~ 25.5 MeV) and magnitude (~ 16 mb) of the major GDR strength. The integrated cross sections derived from each are also in good agreement. The value of the integrated cross section up to 26.5 MeV derived from the cross section shown in Fig. 1(a) is 78 ± 9 MeV mb, and that derived from Fig. 1(b) is 76 ± 7 MeV mb. In view of this consistency, and because of the smaller errors associated with the cross section obtained using the gas sample, the cross section shown in Fig. 1(a) will be used in the discussions which follow.

III. DISCUSSION

A. Comparison with other measurements

One of the original motivations for remeasuring this reaction cross section was to resolve a discrepancy, near 15 MeV, in the magnitudes of the $^{15}\text{N}(\gamma, sn)$ cross section as measured at LLNL (Ref. 2) and the $^{15}\text{N}(\gamma, n_0)$ cross section published by Watson *et al.*³ The ground-state-neutron cross section must be less than or equal to the total photoneutron cross section; yet in contradiction with this, the $^{15}\text{N}(\gamma, n_0)$ cross section³ reaches a maximum of 2.6 mb while the $^{15}\text{N}(\gamma, sn)$ cross section from LLNL (Ref. 2) goes through a minimum of about 1.5 mb. At energies below 14 MeV the LLNL data, although generally lower than the (γ, n_0) , are statistically consistent with it. The present data in this same energy region, while statistically consistent with the LLNL data, are generally higher around 15 MeV and hence in essential agreement with the $^{15}\text{N}(\gamma, n_0)$ results of Watson *et al.* The $^{14}\text{N}(n, \gamma_0)$ results of Wender *et al.*,⁴ which following detailed balance can be directly compared with the (γ, n_0) cross section of Watson *et al.*, are generally higher. However, the recent data by Lafontaine *et al.*¹⁰ of the $^{14}\text{N}(n, \gamma_0)$ reaction, at $E_n = 11$ MeV, do not contradict the work of Watson *et al.* We therefore suggest that around 15 MeV, the LLNL data are slightly low. On the other hand, the fact that below 14 MeV the (γ, n_0) cross section is generally larger than the present $^{15}\text{N}(\gamma, n)$ (and the LLNL data) should be considered. The possibility that (at least at low energies) the (γ, n_0) cross section of Watson *et al.* is too large, or the present results too small, should not be dismissed.

The other region where this measurement disagrees with the earlier work of Jury *et al.*² is in the region of the GDR. Firstly, at an excitation energy of 23 MeV there is no evidence in the present data of the peak seen in the LLNL data; the present cross section rises smoothly from a small valley at about 23 MeV to a maximum at 25 MeV. The explanation of this variance is likely to be found in an underestimate of the efficiency for detecting neutrons emitted from states in ^{15}N in this excitation region. The efficiency of the LLNL detector is dependent on the neutron energy in a known way, and has been calibrated using neutron sources of known average energy.¹¹ In order to determine the efficiency for a particular point in an experiment, the average neutron energy is estimated from the ratio of the number of neutrons detected in the inner and outer rings of BF_3 proportional counters that

constitute the detector. The statistics on this ratio are often poor and, as can be seen in Fig. 3 of Ref. 12 the data points at some energies can scatter significantly about the smooth line used to determine the efficiency.

In the region of 23 MeV the disagreement between the present measurement and that of Jury *et al.* can be explained in terms of an incorrect estimate of the efficiency of the neutron detector. From Fig. 2 of Ref. 2 it can be seen that the curve drawn as an estimate of the average neutron energy shows a considerable excursion in the region of photon energies near 23 MeV. An incorrectly high value for the average neutron energy from this curve would lead to an efficiency that was too low and a cross section that was artificially high. It is suggested that the disagreement between the two measurements in this energy region is a consequence of an overestimation by Jury *et al.* of the average neutron energy.

It is worth noting in passing that when a neutron detector with an energy-dependent efficiency, such as that used at LLNL, is used to determine photoneutron cross sections for light nuclei, extreme care must be taken in determining the efficiency. In such nuclei the paucity of low-lying residual states can lead to significant and rapid variations in the average neutron energy as new decay channels open. Evidence of such an effect is reported by McNeill *et al.*¹³ for the $^{29}\text{Si}(\gamma, n)$ cross section. For studies on heavy nuclei, the average neutron energy is relatively constant, and the possibility of amplifying or diminishing structure due to fluctuations in the detector efficiency is unlikely.

The largest and possibly the most significant disagreement between this measurement of the $^{15}\text{N}(\gamma, n)$ cross section and that of Jury *et al.* occurs at 25.5 MeV. Although both measurements indicate a major peak in this region, the present results give a magnitude of about 16 mb compared to only 9 mb according to LLNL data. There is no apparent explanation for this clear and significant disagreement. It seems unlikely that Jury *et al.* could overestimate the efficiency in this region by nearly a factor of 2. On the other hand the present results from two measurements using different samples confirm the larger value of the cross section. The neutron detector at Melbourne is common to both the present measurements. As mentioned earlier, its efficiency is constant within 10% for neutrons from 0.5 to 10 MeV, and the evidence from Ref. 2 is that the average neutron energy lies well within this range. The implications of the differences between the $^{15}\text{N}(\gamma, sn)$ cross section reported here and that by Jury *et al.* will be discussed below.

B. Isospin considerations

$E1$ absorption in non-self-conjugate nuclei, with ground-state isospin T_0 , leads to excited states with isospin T_0 and $T_0 + 1$. These GDR states are generally referred to as the $T_<$ and $T_>$ components, respectively. A number of authors¹⁴⁻¹⁷ have developed expressions that describe the relative positions and the integrated strengths of these two components. In order to compare the predictions of these expressions with experiment, it is

necessary to identify the isospin components of the photoabsorption cross section of ^{15}N .

Decay from excited states of ^{15}N , whether by neutron or proton emission, satisfies a selection rule such that the change in isospin between the initial and final states is $\Delta T = \pm \frac{1}{2}$. The relative strengths of the allowed decay modes are characterized by Clebsch-Gordan coupling coefficients. Figure 2 shows the relevant level information for the $^{15}\text{N}(\gamma, n)$ and the $^{15}\text{N}(\gamma, p)$ reactions. The ratio of these cross sections can provide an indication of the isospin of the GDR states of ^{15}N .

Additional isospin information can be determined from the $^{15}\text{N}(\gamma, n_0)$,³ and $^{15}\text{N}(\gamma, 2n)$ (Ref. 9) reaction cross sections, together with the $^{15}\text{N}(\gamma, \gamma')$ work of Patrick *et al.*¹⁸ The $^{15}\text{N}(\gamma, n_0)$ reaction can only proceed from $T_<$ states in ^{15}N , so it will indicate only $T = \frac{1}{2}$ strength. Discussion of the $^{15}\text{N}(\gamma, 2n)$ cross section in Ref. 9 sheds some light on the isospin distribution above 20 MeV, while the information as to the population of states in the mass-14 nuclei obtained from the $^{15}\text{N}(\gamma, \gamma')$ data also helps in making isospin assignments to the ^{15}N -GDR states.

As no high resolution measurement of the $^{15}\text{N}(\gamma, p)$ cross section has been reported, a composite cross section was created using the $^{15}\text{N}(\gamma, p)$ cross section measurement by Denisov *et al.*¹⁹ and, in the low-energy region, a cross section determined from the inverse $^{14}\text{C}(p, \gamma_0)$ reaction by Harakeh *et al.*,²⁰ using detailed balance. The composite $^{15}\text{N}(\gamma, p)$ cross section that will be used in the following discussion is shown in Fig. 3.

1. Structure near threshold

The thresholds for the photoneutron and photoproton reactions in ^{15}N are very similar, 10.83 and 10.20 MeV, respectively, so that intercomparison of the strengths of these two decay channels can be made over essentially the entire photoabsorption cross section. The photoproton cross section, shown in Fig. 3, has a resonance just

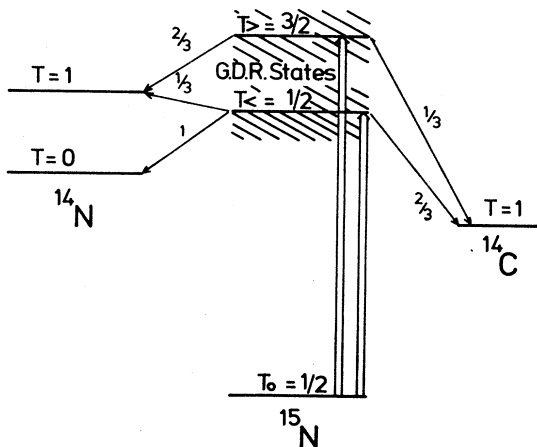


FIG. 2. The Clebsch-Gordan coupling coefficients between the excited $T = \frac{1}{2}$ and $T = \frac{3}{2}$ GDR states in ^{15}N and the $T = 0$ and $T = 1$ residual states in ^{14}N and ^{14}C . The $T = 2$ states are not kinematically accessible in ^{14}N or ^{14}C (Ref. 21).

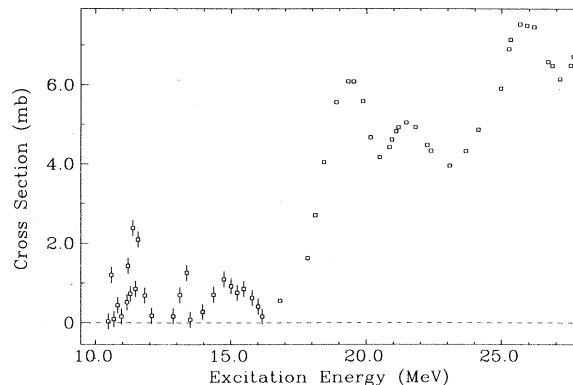


FIG. 3. The $^{15}\text{N}(\gamma, p)$ cross section compiled from the data of Denisov *et al.* (Ref. 19) above 16.3 MeV and the $^{15}\text{N}(\gamma, p_0)$ data from Harakeh and Kuan. There is a systematic uncertainty of about 20% above 16.3 MeV.

above threshold, at about 11.5 MeV. A similar but more pronounced resonance is seen at 11.8 MeV in the photoneutron cross section. Because these two features are very close in energy, they might be considered to be due to the same state in ^{15}N . However, there is evidence that this is not so, and it can be shown that the differences in the $^{15}\text{N}(\gamma, p)$ and $^{15}\text{N}(\gamma, n)$ cross sections result from isospin effects.

Ajzenberg-Selove²¹ reports evidence of a fairly broad ($J = \frac{1}{2}^+$, $T = \frac{3}{2}$, $\Gamma = 405$ keV) state at 11.62 MeV in ^{15}N , which is clearly seen in the $^{14}\text{C}(p, \gamma_0)$ reaction²² and should consequently be seen in the $^{15}\text{N}(\gamma, p)$ cross section. Neutron emission from this state to the only available ($T = 0$, ground) state in ^{14}N is forbidden by isospin selection rules and, despite the 3.5-MeV Coulomb barrier, proton emission is preferred. On the other hand the feature in the photoneutron cross section at 11.8 MeV, evidence of which is not seen in the photoproton cross section, nor in the $^{14}\text{C}(p, \gamma_0)$ inverse reaction, must be due to the decay of a $T_<$ state, or group of states, in ^{15}N ; all neutron decay in this energy region must be to the $T = 0$ ground state of ^{14}N . Ajzenberg-Selove²¹ includes three candidates with spins accessible to $E1$ excitation, and parities either positive or unassigned. These states at 11.78 ($\frac{3}{2}^+$), 11.88 ($\frac{3}{2}$), and 11.97 MeV ($\frac{1}{2}$), if responsible for the observed structure in the $^{15}\text{N}(\gamma, n)$ cross section, must have isospin of $\frac{1}{2}$, and this should be noted in the compilation.

In the excitation energy region from 12 to 13.5 MeV both the $^{15}\text{N}(\gamma, n)$ and $^{15}\text{N}(\gamma, p)$ cross sections are small. This is probably related to the fact that levels in this region of ^{15}N are not accessible (Ref. 21) to $E1$ transitions from the ^{15}N ground state.

From 13.5 to 15.5 MeV the $^{15}\text{N}(\gamma, n_0)$ and $^{15}\text{N}(\gamma, n)$ cross sections are in agreement within the stated errors. This indicates that all states seen in the $^{15}\text{N}(\gamma, n)$ reaction channel up to 15 MeV have an isospin of $\frac{1}{2}$; at these energies, well above the photoproton threshold (10.2 MeV), $T = \frac{3}{2}$ states are forbidden to decay to the ($T = 0$) ground state of ^{14}N .

In this energy region there is a correspondence in the features of the $^{15}\text{N}(\gamma, n)$ and $^{15}\text{N}(\gamma, p)$ cross sections; in particular, relatively broad peaks at about 14.7 and 15.4 MeV are seen in both cross sections. Harakeh *et al.*²⁰ tentatively assigned to states at these energies spins and parities of $\frac{1}{2}^+$ and $\frac{3}{2}^+$ with widths of about 750 keV. It is now possible, in view of the argument above, to assign them an isospin value at $T = \frac{1}{2}$.

2. The region from 16 to 20 MeV

Above 16 MeV the $^{15}\text{N}(\gamma, n)$ cross section rises to a peak at 17.7 MeV, while the $^{15}\text{N}(\gamma, p)$ cross section remains quite small. The relative increase of the $^{15}\text{N}(\gamma, n)$ cross section results from some five additional $T=0$ states in ^{14}N becoming accessible for neutron decay, while for protons the only decay that is unimpeded by the Coulomb barrier is that to the ground state. The population of these nonground states in ^{14}N is confirmed by the fact that the $^{15}\text{N}(\gamma, n_0)$ cross section as reported in Ref. 3 constitutes only a fraction of the total $^{15}\text{N}(\gamma, n)$ cross section. This dissimilarity in level densities in the two residual nuclei leads to dominance of the photoneutron cross section. It should be noted that this explanation implies that the ^{15}N states in this energy region are predominantly $T_<$, since if they were $T_>$ states, neutron decay could not only occur to the single $T=1$ state at 2.31 MeV in ^{14}N , and would be comparable in strength to the only unimpeded proton decay to the ground state in ^{14}C .

The strength in this region may be attributed to three states reported in Ref. 21. The first is at 16.667 MeV ($\frac{1}{2}^+, \frac{1}{2}$), followed by two states very close to each other, one at 17.58 MeV ($\frac{3}{2}^+, \Gamma=450$ keV) and the second at 17.67 MeV ($\frac{3}{2}^+, \frac{1}{2}, \Gamma=600$ keV). The suggestion that these three states are all $T_<$ in nature is supported by the observation of significant strength at energies corresponding to these states in the $^{11}\text{B}(\alpha, \gamma_0)^{15}\text{N}$ cross section as measured by Degré *et al.*²³

From about 17 MeV, the $^{15}\text{N}(\gamma, p)$ cross section rises smoothly to a peak of about 6 mb at 19.4 MeV. In contrast, over the same energy range the $^{15}\text{N}(\gamma, n)$ cross section decreases to a minimum at 18.7 MeV, such that between 18 and 20 MeV photoproton decay actually exceeds photoneutron decay. Although this dominance of photoproton decay is not a direct consequence of isospin, it does allow an isospin assignment of $T = \frac{3}{2}$ to be made to states in this energy region of ^{15}N . Ignoring all other factors such as residual-state density and Coulomb effects, photoneutron decay from any of the kinematically accessible states in ^{15}N , irrespective of its isospin, is expected to exceed photoproton decay by a factor of 2 consistent with the Clebsch-Gordan coupling coefficients as shown in Fig. 2. This expectation is in contradiction with the experimental facts. However, if a $T = \frac{3}{2}$ assignment is made, the effect of residual-state density becomes very important. Neutron decay is forbidden to $T=0$ states in ^{14}N , whereas proton decay is possible to any of the energetically accessible states in ^{14}C . Over most of this energy region neutron decay is possible to only one

$T=1$ state (2.31 MeV) in ^{14}N ; a second one (8.1 MeV) becomes accessible only at excitations in ^{15}N above 18.9 MeV. On the other hand the number of proton-accessible states in ^{14}C which are essentially Coulomb-uninhibited increases from one to seven. This disparity in the number of available residual states, when considered in conjunction with predominantly $T = \frac{3}{2}$ strength in this energy region of the ^{15}N GDR, could produce the observed dominance of proton decay. At higher energies the disparity in the number of available states in ^{14}C and ^{14}N disappears, and the neutron decay channel again dominates.

The presence of $T_>$ strength in ^{15}N at about 18 MeV is confirmed by the deexcitation γ -ray studies of Patrick *et al.*¹⁸ who show that the first $T=1$ state in ^{14}N (2.31 MeV) begins to be populated at about 18 MeV. There is of course still considerable $T_<$ strength in this region of the ^{15}N GDR, as indicated by both the population of the $T=0$ (3.95 MeV) state reported in Ref. 18 and the significant ground-state neutron cross section.³

Similarly in the proton decay channel evidence of population of states other than the ground state can be seen in the work of Patrick *et al.*¹⁸ Comparison of the $^{15}\text{N}(\gamma, p_0)$ cross section (derived from the proton capture measurements of Harakeh *et al.*²⁰ and Rhodes and Stephens²⁴) with the total photoproton cross section, shown in Fig. 3, indicates that just below 20 MeV more than 50% of proton decays are to excited states in ^{14}C . It might be noted that this fraction of excited-state decay, derived as it is from the work of Denisov,¹⁹ is not consistent with the more recent, though more poorly resolved, deexcitation studies of Patrick *et al.*¹⁸ Nonetheless there is an observed increase in number of proton decays from ^{15}N to ^{14}C . This observation is consistent with the explanation advanced above, that in this energy region there is a dominance of $T_>$ excited states in ^{15}N .

The above arguments are consistent with the known dipole states in this energy region as reported in Ref. 21. A state at 19.5 MeV is suggested by Harakeh *et al.*²⁰ to have $T = \frac{3}{2}$; the absence of a noticeable peak at this energy in the $T_<$ -selective $^{15}\text{N}(\gamma, d_0)$ reaction cross section measured by Skopik *et al.*²⁵ reinforces this isospin assignment. Another state reported in Ref. 21 at 20.5 MeV, with $J = \frac{3}{2}^+$ but no assigned isospin, must also have $T = \frac{3}{2}$, being unobserved in the $^{15}\text{N}(\gamma, d_0)$ cross section, which approaches a minimum at ≈ 20.5 MeV.

3. The region from 20 to 26 MeV

The $^{15}\text{N}(\gamma, n)$ cross section is seen to rise smoothly from a magnitude of 5 mb at 20 MeV to about 6.5 mb at 23 MeV, with a dip back to 6 mb at 23.5 MeV. The magnitude then rises quickly to a GDR maximum of ≈ 16 mb at 25.5 MeV. There is general agreement between the shapes of the $^{15}\text{N}(\gamma, p)$ and $^{15}\text{N}(\gamma, n)$ cross sections from 20 to 24 MeV. However, the $^{15}\text{N}(\gamma, n)$ cross section becomes increasingly dominant above 24 MeV.

Evidence about the isospin nature of the excited dipole states of ^{15}N in this energy region can be deduced from the $^{15}\text{N}(\gamma, 2n)$ cross section which has a reaction threshold at 21.8 MeV. In contrast to the general shape of

$(\gamma, 2n)$ reactions in other light nuclei, which rise smoothly from threshold, the $^{15}\text{N}(\gamma, 2n)$ cross section stays close to zero for about 3 MeV above threshold, and then begins to rise at around 24 MeV. McNeill *et al.*⁹ have interpreted this behavior as indicating the dominance of $T = \frac{3}{2}$ states in this energy region of the ^{15}N GDR. It should be noted, however, that the presence of strength in the $^{15}\text{N}(\gamma, n_0)$ channel³ up to 26 MeV confirms the presence of a small and decreasing $T_<$ component.

Consistent with the above conclusions it is possible to identify tentatively the various states contributing in this energy region. At 21.8 MeV a broad peak is clearly seen in the $T_<$ -selective $^{15}\text{N}(\gamma, d_0)$ reaction channel,²⁵ identifying at least part of the $T = \frac{1}{2}$ dipole strength in this region. Peaks seen in the $^{14}\text{C}(p, \gamma_0)$ (Ref. 20) at 23 and 25.5 MeV correspond to strength seen in the present $^{15}\text{N}(\gamma, n)$ cross section, whilst the absence of structure in the $^{15}\text{N}(\gamma, d_0)$ cross section supports the assertion that they have isospin $T = \frac{3}{2}$.

At this point it is relevant to discuss the significant difference at 25.5 MeV in the $^{15}\text{N}(\gamma, n)$ reaction cross section presented here and that of Jury *et al.*² The $^{15}\text{N}(\gamma, n)$ cross section has a peak value of close to 16 mb at 25.5 MeV. At excitation energies from 25 to 26 MeV there are many residual states accessible for both neutron and proton decay, and the Coulomb barrier is substantially overcome. If all else is equal, the Clebsch-Gordan coefficients obtained from the isospin coupling of the excited and residual states will now give a good measure of the fraction of decays expected to the various states (see Fig. 2); and hence should give a reliable estimate of the ratio of the $^{15}\text{N}(\gamma, p)$ to the $^{15}\text{N}(\gamma, n)$ cross section.

Figure 2 shows that when many states (both $T_<$ and $T_>$) are available in the residual nuclei, the expected $(\gamma, n)/(\gamma, p)$ ratio is 2, independent of the isospin of the excited state in ^{15}N . Although in this case the $(\gamma, n)/(\gamma, p)$ ratio does not yield any information about the isospin of the excited states, when there are many residual states it gives a clear indication of the expected magnitude of the $^{15}\text{N}(\gamma, n)$ cross section relative to that of the $^{15}\text{N}(\gamma, p)$. If the ratio is taken of the $^{15}\text{N}(\gamma, n)$ cross section reported by Jury *et al.*² to the $^{15}\text{N}(\gamma, p)$ cross section as measured by Denisov at an energy of about 25 MeV, a value of approximately one is obtained. In contrast, at 25 MeV, the magnitude of the $^{15}\text{N}(\gamma, n)$ cross section presented here is about twice that of Denisov, so that the ratio $^{15}\text{N}(\gamma, n)/^{15}\text{N}(\gamma, p)$ is of the order of 2, in reasonably good agreement with the predicted value. It should be noted that the uncertainties associated with the Denisov data in this energy region are quite large and thus there must also be a large uncertainty in the ratios just mentioned. However, these ratios tend to support the contention made earlier that the magnitude of the present measurement is correct and the $^{15}\text{N}(\gamma, n)$ measurement of Jury *et al.* may have been seriously underestimated at about 25.5 MeV.

4. Separation of $T_<$ and $T_>$ GDR components

The discussion above leads to fairly complete isospin assignments for the structure in the photoabsorption

cross section of ^{15}N . Using this basis it is possible to obtain an approximation to the $T_<$ and $T_>$ components of the GDR. This can be done by fitting the total photoabsorption cross section with a series of resonances, with known isospin and energies as noted above. As an approximation to the total photoabsorption cross section, needed for this process, the sum of the $^{15}\text{N}(\gamma, sn)$ cross section reported here plus the composite $^{15}\text{N}(\gamma, p)$ cross section shown in Fig. 3 was used. It was assumed that contributions from other decay modes were negligible. This cross section is shown in Fig. 4. The error bars indicate the statistical uncertainty arising from the $^{15}\text{N}(\gamma, sn)$ cross section only. Above 16 MeV there may be an increasing systematic error due mainly to uncertainties in the $^{15}\text{N}(\gamma, p)$ data of Denisov *et al.*,¹⁹ which may amount to an overestimate at 28 MeV of up to 20%.

In the least-squares-fitting procedure the levels identified in the discussion above were used. A Lorentz function was used for each resonance, and the fit to the absorption cross section was optimized by adjusting the height, keeping the energy and width within limits consistent with those mentioned above. The resulting fit is shown in Fig. 4 together with the absorption cross section. The agreement is remarkable. Table I lists the parameters associated with the fit, combined into $T = \frac{1}{2}$ and $T = \frac{3}{2}$ states. The widths listed are generally larger than those of the states discussed above, and reflect to some extent the resolution of the experimental data.

It is now relatively straightforward to collect the isospin components of the cross section together. Figure 5 shows the $T_<$ and $T_>$ components of the GDR resulting from the fitting procedure.

In estimating the energy splitting and integrated cross sections of the two isospin components of the GDR, we have used the fitted curves of Fig. 5, up to an energy of 40 MeV, even though the data presented here extends only to 26.5 MeV. This is consistent with the observation of Jury *et al.*² that there is no significant structure seen between 28 and 40 MeV. On this basis the values of the energy weighted integrated cross sections for the two components are

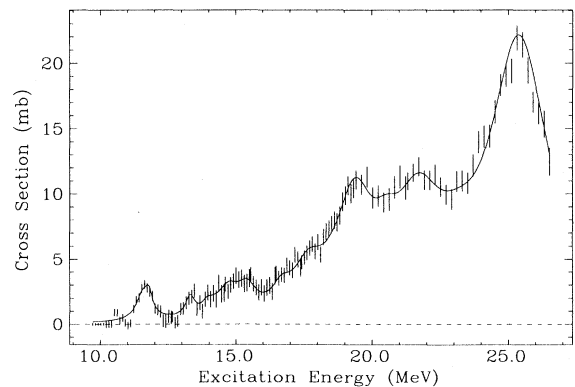


FIG. 4. The total photoabsorption cross section approximated from the $^{15}\text{N}(\gamma, n)$ plus $^{15}\text{N}(\gamma, p)$ cross sections, as described in the text. The solid line is obtained by fitting the data with $E1$ absorption to possible states identified in the text.

TABLE I. The contribution of $E1$ -accessible states to the GDR in ^{15}N . The contributions were obtained by a fitting procedure as described in the text.

Energy (MeV)	Width (MeV)	Strength (MeV mb)
$T = \frac{1}{2}$ transitions		
11.78	0.30	0.65
13.30	0.40	0.93
13.90	0.40	0.31
14.10	0.61	0.38
14.71	1.03	3.14
15.40	0.80	2.10
16.68	0.80	1.61
17.67	1.40	6.42
18.91	1.70	6.80
19.20	0.80	1.13
21.70	2.20	24.85
$T = \frac{3}{2}$ transitions		
11.55	0.60	1.81
19.50	1.40	12.13
20.50	1.20	4.72
23.19	2.00	6.61
25.40	2.60	78.76

$$\sigma_{-1}(T = \frac{1}{2}) = 2.51 \text{ mb},$$

$$\sigma_{-1}(T = \frac{3}{2}) = 4.40 \text{ mb}.$$

This gives an experimental value for $\sigma_{-1}(T = \frac{3}{2}) / \sigma_{-1}(T = \frac{1}{2} + T = \frac{3}{2})$ of 0.64. The comparison with the theoretical predictions of Ref. 14, which gives 0.55, and Ref. 15, which gives 0.61, is extremely good.

The splitting, ΔE , of the two isospin components of the GDR of ^{15}N following this analysis is 4.4 MeV, where ΔE is defined as

$$\Delta E = \frac{\int \sigma(T+1)dE}{\int \sigma(T+1)dE/E} - \frac{\int \sigma(T)dE}{\int \sigma(T)dE/E}.$$

According to both Akyuz and Fallieros¹⁶ and Leonardi,¹⁵ the predicted splitting is given by

$$\Delta E = (T_0 + 1)U/A,$$

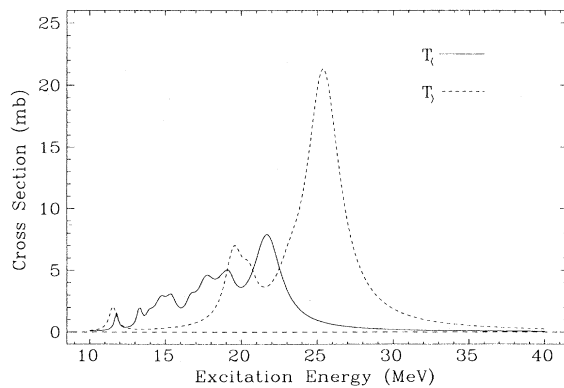


FIG. 5. The $T = \frac{1}{2}$ and $T = \frac{3}{2}$ isospin components of the ^{15}N GDR.

where T_0 is the ground-state isospin of a nucleus of mass number A , and U is the symmetry energy. Akyuz and Fallieros, using a value of $U = 60$ MeV, predict a splitting of 6.0 MeV, whereas Leonardi¹⁵ calculated the symmetry energy for ^{15}N to have a value of $U = 14$ MeV, which leads to a predicted splitting of 1.4 MeV. Neither value is in particularly good agreement with the experimental value, and it is proposed that reconciliation is brought about if the symmetry energy is 46 MeV.

The question as to whether the symmetry energy as used in the derivations above is constant was one aspect of a study of isospin effects in medium-mass nuclei that was carried out in this laboratory.²⁶ The summary of data presented in Ref. 27, and in particular Fig. 10 of that reference, indicates that a value of less than 60 MeV for the symmetry energy would fit the experimental results better.

C. Comparison with theory

Although it is not anticipated that theoretical calculations of the photoabsorption cross section of ^{15}N will show exact correspondence with the detailed structure revealed in the experimental measurement, the basic assumptions of the calculation might well be tested in such a comparison.

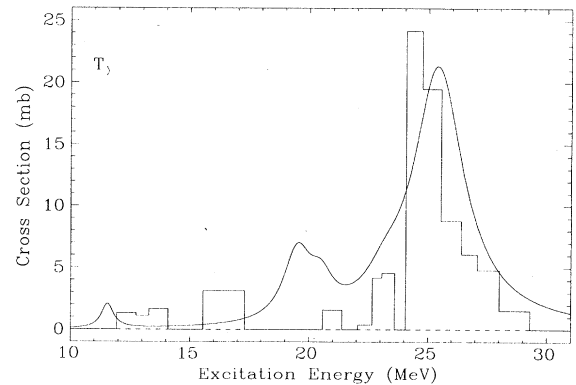
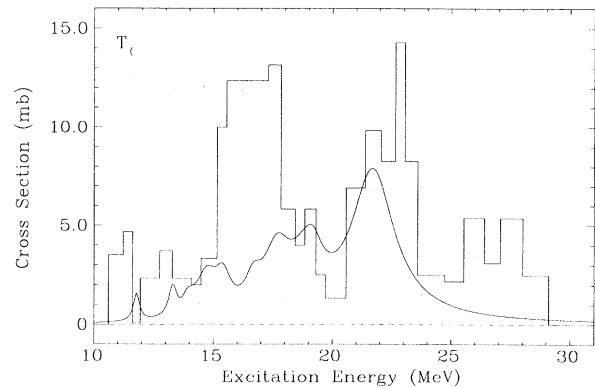


FIG. 6. The calculation of Albert *et al.* (Ref. 28) using the Tabakin interaction compared to the components as derived in the text (see Fig. 5). The upper part of the figure shows the $T_{<}$ dipole states and the lower part the $T_{>}$ states.

Figure 6 shows the approximate photoabsorption cross section derived as described above, and shown first in Fig. 4, together with the calculation by Albert *et al.*²⁸ The calculation considers creation of two-hole one-particle states in ^{15}N by $E1$ excitation. Two calculations are presented, one using a zero-range Soper residual interaction, and the other a separable Tabakin potential. The latter, shown in Fig. 5(a) of Ref. 28 is in better agreement with the measured location and strength distribution shown in the data; however, there is clearly an overestimate of the $T_{<}$ strength. Use of the Soper residual interaction [Fig. 5(b)] results in excess strength in the 22–24 MeV region.

The observation, that the results of the calculation using the Tabakin potential are in better agreement with the experimental data, is in contrast to the situations for ^{13}C (Ref. 29) and ^{17}O (Ref. 30). In both these cases, after renormalization, better agreement was found between the experimental data and calculations performed by Albert *et al.*³¹ using the zero-range Soper potential. It would seem that in ^{15}N , where $2h-1p$ dipole states are involved, the Tabakin potential is more satisfactory; whereas for nuclei like ^{13}C and ^{17}O , where $2p-1h$ excitations dominate, the Soper potential gives more realistic results.

A calculation by Fraser *et al.*³² used two different residual interactions. One was a Gaussian form with spin and isospin exchange as used by Gillet and Vinh-Mau, and the other a zero-range force with Soper spin exchange. A number of different strengths were used for the zero-range force and, as Fig. 2 of Ref. 32 shows, this can move the energy of maximum absorption and vary the distribution of the strength significantly. The Gillet-type residual interaction leads to a result that agrees with experiment, in that strong $T_{>}$ absorption occurs just above 25 MeV, with dominant $T_{>}$ cross section strength between 21 and 25 MeV, while $T_{<}$ states concentrate between 17 and 21 MeV. The comparison is shown in Fig. 7.

Despite the overall agreements mentioned above, which are interpreted as indications as to the validity of the potentials chosen in the calculations, it is not surprising that close correlations between theory and experiment are not seen. Other important model assumptions will affect the $E1$ absorption strength and distribution. The provision of reliable experimental data should provide a basis for more sophisticated calculations which might hope to clarify the nature of the model bases.

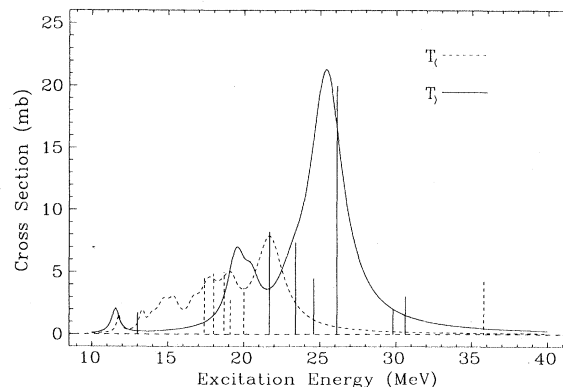


FIG. 7. The $T_{<}$ (dashed) and $T_{>}$ (solid) components of the GDR as calculated by Fraser *et al.* (Ref. 32) using the Gillet potential, compared with the isospin components as resolved in the text.

IV. CONCLUSIONS

This paper has attempted to provide reliable data on the photodisintegration of ^{15}N , one of the significant members in a systematic study of nuclei with one particle or hole outside a closed shell. This measurement suggests possible resolution of a number of discrepancies evidenced in earlier data. We suggest that the $^{15}\text{N}(\gamma, n)$ cross section as reported by Jury *et al.*² may be underestimated in the region of 15 MeV. Both measurements of the cross section presented here agree that the major GDR strength occurs at 25.5 MeV rather than 23.5 MeV as reported in the measurement by Jury *et al.*²

A careful reconciliation of the observed structure in the cross section with known $E1$ -accessible states in ^{15}N provided a basis that allowed the cross section to be resolved into its two isospin components. The relative bremsstrahlung-weighted integrated cross section of these components is in good agreement with calculated values. The observed isospin splitting of these GDR components is only consistent with the theoretical predictions if the symmetry energy used in the calculations is reduced from the value of 60 to 46 MeV for this nucleus.

This cross section, when compared to shell-model calculations, confirms the observation of Jury *et al.*² that ^{15}N with GDR configurations that are predominantly $1p-2h$ is not well explained by a Soper mixture of exchange forces.

¹R. E. Pywell, B. L. Berman, J. G. Woodworth, J. W. Jury, K. G. McNeill, and M. N. Thompson, Phys. Rev. C **32**, 384 (1985).

²J. W. Jury, B. L. Berman, J. G. Woodworth, M. N. Thompson, R. E. Pywell, and K. G. McNeill, Phys. Rev. C **26**, 777 (1982).

³J. D. Watson, J. W. Jury, P. C.-K. Kuo, W. F. Davidson, N. K. Sherman, and K. G. McNeill, Phys. Rev. C **27**, 506 (1983).

⁴S. A. Wender, H. R. Weller, N. R. Roberson, D. R. Tilley, and R. G. Seyler, Phys. Rev. C **25**, 89 (1982).

⁵R. J. Hughes, R. H. Sambell, E. G. Muirhead, and B. M. Spicer, Nucl. Phys. **A238**, 189 (1975).

⁶T. S. Pruitt and S. R. Domen, Natl. Bur. Stand. (U.S.) Monogr.

48 (1962).

⁷E. L. Bramanis, T. K. Deague, R. S. Hicks, E. G. Muirhead, R. H. Sambell, and R. J. J. Stewart, Nucl. Instrum. **100**, 59 (1972).

⁸R. E. Pywell, M. N. Thompson, and B. L. Berman, Nucl. Instrum. **178**, 149 (1980).

⁹K. G. McNeill, A. D. Bates, R. P. Rassool, E. A. Milne, and M. N. Thompson, Phys. Rev. C **37**, 1403 (1988).

¹⁰J. R. C. Lafontaine, J. W. Jury, H. R. Weller, N. R. Roberson, and D. R. Tilley, in *Sigtuna Workshop on Radiative Capture*, edited by E. Nilsson (University of Uppsala, Uppsala, 1987).

¹¹D. D. Faul, B. L. Berman, P. Meyer, and D. L. Olsen, Phys.

- Rev. C **24**, 849 (1981).
- ¹²B. L. Berman, J. T. Caldwell, R. R. Harvey, M. A. Kelly, R. L. Bramblett, and S. C. Fultz, Phys. Rev. **162**, 1098 (1967).
- ¹³K. G. McNeill, R. E. Pywell, B. L. Berman, J. G. Woodworth, M. N. Thompson, and J. W. Jury, Phys. Rev. C **36**, 1621 (1987).
- ¹⁴Evans Hayward, B. F. Gibson, and J. S. O'Connell, Phys. Rev. C **5**, 846 (1972).
- ¹⁵R. Leonardi, Phys. Rev. Lett. **28**, 836 (1972).
- ¹⁶R. O. Akyuz and F. Fallieros, Phys. Rev. Lett. **27**, 1016 (1971).
- ¹⁷F. Fallieros and B. Goulard, Nucl. Phys. **A147**, 593 (1970).
- ¹⁸B. H. Patrick, E. M. Bowey, and E. G. Muirhead, J. Phys. G **2**, 751 (1976).
- ¹⁹V. P. Denisov, L. A. Kul'chitski, and I. Ya. Chubukov, Yad. Fiz. **14**, 889 (1971) [Sov. J. Nucl. Phys. **14**, 497 (1972)].
- ²⁰M. H. Harakeh, P. Paul, H. M. Kuan, and E. K. Warburton, Phys. Rev. C **12**, 1410 (1975).
- ²¹F. Ajzenberg-Selove, Nucl. Phys. **A449**, 1 (1986).
- ²²H. M. Kuan, C. J. Umbarger, and D. G. Shirk, Nucl. Phys. **A160**, 211 (1971).
- ²³A. Degré, M. Schaffer, G. Bonneaud, and I. Linck, Nucl. Phys. **A306**, 77 (1978).
- ²⁴Jacob L. Rhodes and W. E. Stephens, Phys. Rev. **110**, 1415 (1958).
- ²⁵D. M. Skopik, J. J. Murphy II, H. R. Weller, R. A. Blue, N. R. Roberson, S. A. Wender, and D. R. Tilley, Phys. Rev. C **20**, 409 (1979).
- ²⁶J. W. Norbury, M. N. Thompson, K. Shoda, and H. Tsubota, Aust. J. Phys. **31**, 471 (1978); R. E. Pywell and M. N. Thompson, Nucl. Phys. **A318**, 461 (1979); R. E. Pywell, M. N. Thompson, and R. A. Hicks, *ibid.* **A325**, 116 (1979); R. Sutton, M. N. Thompson, M. Sugawara, K. Shoda, T. Saito, and H. Tsubota, *ibid.* **A339**, 125 (1980); R. E. Pywell, M. N. Thompson, K. Shoda, M. Sugawara, T. Saito, H. Tsubota, H. Miyase, J. Uegaki, T. Tamae, H. Ohashi, and T. Urano, Aust. J. Phys. **33**, 685 (1980); Y. I. Assafiri and M. N. Thompson, Nucl. Phys. **A357**, 429 (1981); P. D. Harty and M. N. Thompson, Aust. J. Phys. **34**, 505 (1981); G. J. O'Keefe, M. N. Thompson, Y. I. Assafiri, and K. Shoda, Nucl. Phys. **A469**, 239 (1987).
- ²⁷M. N. Thompson, in *Nuclear Interactions*, Vol. 92 of *Lecture Notes in Physics*, edited by B. Robson (Springer-Verlag, Berlin, 1979), p. 208.
- ²⁸D. J. Albert, J. George, and H. Uberall, Phys. Rev. C **16**, 2452 (1977).
- ²⁹D. Zubanov, R. A. Sutton, M. N. Thompson, and J. W. Jury, Phys. Rev. C **27**, 1957 (1983).
- ³⁰J. W. Jury, B. L. Berman, D. D. Faul, P. Meyer, and J. G. Woodworth, Phys. Rev. C **21**, 503 (1980).
- ³¹D. J. Albert, A. Nagl, J. George, R. F. Wagner, and H. Uberall, Phys. Rev. C **16**, 503 (1977).
- ³²R. F. Fraser, R. K. Garnsworthy, and B. M. Spicer, Nucl. Phys. **A156**, 489 (1970).